ACADEMIC PRESS

Available online at www.sciencedirect.com
SCIENCE DIRECT®

VIROLOGY

Virology 311 (2003) 28–39
www.elsevier.com/locate/yviro

Extensive immune-mediated hippocampal damage in mice surviving infection with neuroadapted Sindbis virus

Takashi Kimura[1] and Diane E. Griffin*

W. Harry Feinstone Department of Molecular Microbiology and Immunology, Johns Hopkins Bloomberg School of Public Health, Baltimore, MD 21205, USA

Received 25 July 2002; returned to author for revision 4 December 2002; accepted 16 December 2002

Abstract

Viral infections of the central nervous system and immune responses to these infections cause a variety of neurological diseases. Infection of weanling mice with Sindbis virus causes acute nonfatal encephalomyelitis followed by clearance of infectious virus, but persistence of viral RNA. Infection with a neuroadapted strain of Sindbis virus (NSV) causes fatal encephalomyelitis, but passive transfer of immune serum after infection protects from fatal disease and infectious virus is cleared. To determine whether persistent NSV RNA is associated with neurological damage, we examined the brains of recovered mice and found progressive loss of the hippocampal gyrus, adjacent white matter, and deep cerebral cortex associated with mononuclear cell infiltration. Mice deficient in $CD4^+$ T cells showed less tissue loss, while mice lacking $CD8^+$ T cells showed lesions comparable to those in immunocompetent mice. Mice deficient in both $CD4^+$ and $CD8^+$ T cells developed severe tissue loss similar to immunocompetent mice and this was associated with extensive infiltration of macrophages. The number of $CD4^+$ cells and macrophage/microglial cells, but not $CD8^+$ cells, infiltrating the hippocampal gyrus was correlated with the number of terminal deoxynucleotidyltransferase-mediated dUTP nick end-labeling positive pyramidal neurons. These results suggest that $CD4^+$ T cells can promote progressive neuronal death and tissue injury, despite clearance of infectious virus.

Keywords: Encephalitis; Immunity; Central nervous system; Hydrocephalus; Alphavirus

Introduction

Sindbis virus (SV), an alphavirus in the family *Togaviridae*, infects neurons and causes acute encephalomyelitis in mice. Infection with the prototype AR339 strain of SV causes fatal disease in suckling mice, but not in weanling mice (Taylor et al., 1955; Griffin, 1976; Johnson et al., 1972). Antiviral antibody and interferon-γ play important roles in the clearance of infectious virus from the central nervous system (CNS) of SV-infected weanling mice (Levine et al., 1991; Binder and Griffin, 2001). However, viral RNA and B cells secreting antibody to SV are present in the brains of recovered mice for at least a year after infection (Levine and Griffin, 1992; Tyor et al., 1992), suggesting that virus persists in neurons that survive infection and that some viral proteins may continue to be synthesized long after the resolution of acute encephalitis.

Neuroadapted Sindbis virus (NSV) is a neurovirulent strain of SV that elicits severe, often fatal, encephalomyelitis in adult mice. NSV targets the same neurons as SV but replicates more efficiently, leading to higher viral titers and more widespread infection. Six- to eight-week-old C57BL/6 (B6) mice are highly susceptible to NSV-induced encephalomyelitis and die within 10 days after infection, but a small number of mice infected at older ages survive (Tucker et al., 1996; Kimura and Griffin, 2000). A number of observations suggest that host factors contribute to NSV-induced neuronal death and fatal encephalitis. For instance, BALB/c mice are relatively resistant to fatal disease (Thach et al., 2000),

* Corresponding author. Department of Molecular Microbiology and Immunology, Johns Hopkins Bloomberg School of Public Health, 615 N. Wolfe Street, Baltimore, MD 21205. Fax: +1-410-955-0105.
E-mail address: dgriffin@jhsph.edu (D.E. Griffin).
[1] Present address: Laboratory of Comparative Pathology, Graduate School of Veterinary Medicine, Hokkaido University, Sapporo 060-0818, Japan.

0042-6822/03/$ – see front matter © 2003 Elsevier Science (USA). All rights reserved.
doi:10.1016/S0042-6822(03)00110-7

and in susceptible B6 mice both infected and uninfected neurons die in regions of virus replication (Nargi-Aizenman et al., unpublished observations). A role for the immune response in fatal disease is suggested by the decrease in mortality observed in mice deficient in either β_2-microglobulin or IFN-γ (Kimura and Griffin, 2000; Wesselingh et al., 1994; Rowell and Griffin, 2002). Therefore, NSV infection may damage the CNS both directly by inducing death of infected cells and indirectly as a result of the host immune response to viral proteins.

The process of indirect damage may be prolonged and more severe in mice that do not succumb during the acute phase of infection and may be linked to the persistence of viral RNA in the CNS. For example, immune-mediated demyelination occurs in genetically susceptible mice that survive the acute encephalitic phase of infection with Theiler's murine encephalitis virus or mouse hepatitis virus (Weiner, 1973; Lipton, 1975; Lipton and Dal Canto, 1976). Delayed neuronal damage and tissue loss have been described in animals surviving the acute phase of Semliki Forest, western equine encephalitis, and Borna disease virus infections (Seamer et al., 1971; Zlotnick et al., 1972; Bilzer and Stitz, 1994) and understanding this process could be important for understanding progressive or late neurological disease associated with prior viral infections.

To elucidate the outcome of long-term nonfatal NSV infection, we analyzed the pathologic changes in the brains of 11- to 12-week-old mice surviving acute infection and 6-week-old mice rescued from acute fatal encephalitis by passive transfer of primary immune serum after infection (Griffin and Johnson, 1977; Hirsch et al., 1979; Stanley et al., 1986). These mice had continued damage in the region of the hippocampus after clearance of infectious virus and this was associated with the infiltration of CD4 T cells and macrophages.

Results

NSV infection of highly susceptible B6 mice usually results in fatal encephalomyelitis (Thach et al., 2000), but older animals occasionally survive. To identify long-term pathologic changes associated with NSV infection, surviving mice were examined 60 days after infection (Fig. 1). Surprisingly, these mice had marked destruction of the CA1 and CA2 regions of the hippocampus with extensive loss of brain tissue in the surrounding region creating an intraparenchymal cavity that connected with the ventricular system. The pathogenetic process leading to this outcome was difficult to study since only a small and unpredictable number of mice survived the acute disease. Since passive transfer of immune serum 24-48 h after infection protects BALB/c mice from fatal NSV-induced encephalomyelitis (Stanley et al., 1986; Griffin and Johnson, 1977), we explored the possibility that this experimental system could be used to examine the long-term pathologic consequences of survival from infection with a virulent neuronotropic virus.

To determine whether primary immune serum was sufficient to protect more susceptible B6 mice from fatal NSV encephalitis, B6 mice and immunodeficient B6 mice lacking the recombinase-activating gene 1 (RAG-KO mice) were infected with NSV. There was 100% mortality by day 10 in both B6 and RAG-KO mice infected with NSV (data not shown), but passive transfer of NSV immune serum 24 h after infection protected the majority of mice from fatal encephalitis (Table 1). Mice that survived remained asymptomatic for at least 30 days. Surviving RAG-KO mice developed hindlimb paralysis by 2 months after infection, but B6 mice showed no evidence of neurological disease.

Virus clearance and reappearance after immune serum treatment

The amount of virus in the brains of B6 and RAG-KO mice increased rapidly after infection, with greater than $10^{7.5}$ PFU/g brain present by the time of serum transfer on day 1 (Fig. 2). Maximum virus growth was achieved by day 3 and no difference in peak viral titer was detected between B6 and RAG-KO mice. Infectious virus was rapidly cleared from brains and became undetectable by day 10 in B6 mice and by day 13 in RAG-KO mice treated with immune serum. Infectious virus was again detectable in the brains of RAG-KO mice beginning on day 16 and synthesis of infectious virus reached a plateau by day 25, indicating that virus-infected cells were not eliminated by passive transfer of immune serum. Immunocompetent B6 mice had no reappearance of infectious virus.

In RAG-KO mice, both the enzyme immunoassay (EIA) and the neutralizing antibody titers decreased simultaneously and became undetectable by day 62 as passively transferred antibody decayed (Fig. 3). Neutralizing antibody in B6 mice also decreased after day 16, while antibody measured by EIA continued to increase.

Pathologic changes in the brains of immunocompetent B6 mice and immunodeficient RAG-KO mice

Because primary immune serum effectively protected mice from fatal NSV infection, we anticipated that few pathologic changes would be present in the brains of these mice. However, coronal and midline sagittal sections of brains from B6 mice revealed gross distension of the lateral ventricles as early as 13 days following infection. Ventricular dilation was usually bilateral, although sometimes it was asymmetric. The third and fourth ventricles were normal in size and the amount of cerebrospinal fluid in the subarachnoid space was not excessive. Hydrocephalic changes progressed rapidly, reached an advanced degree by 3 weeks after infection, and were then stable. No mice developed macrocephaly.

To understand the pathologic changes more precisely, we

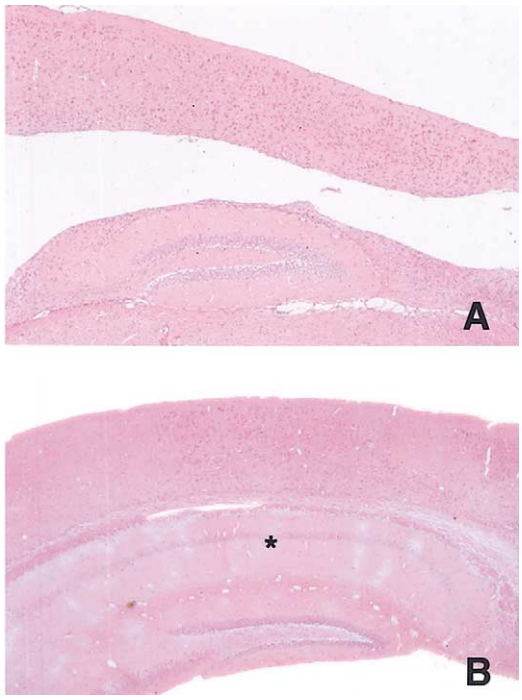

1

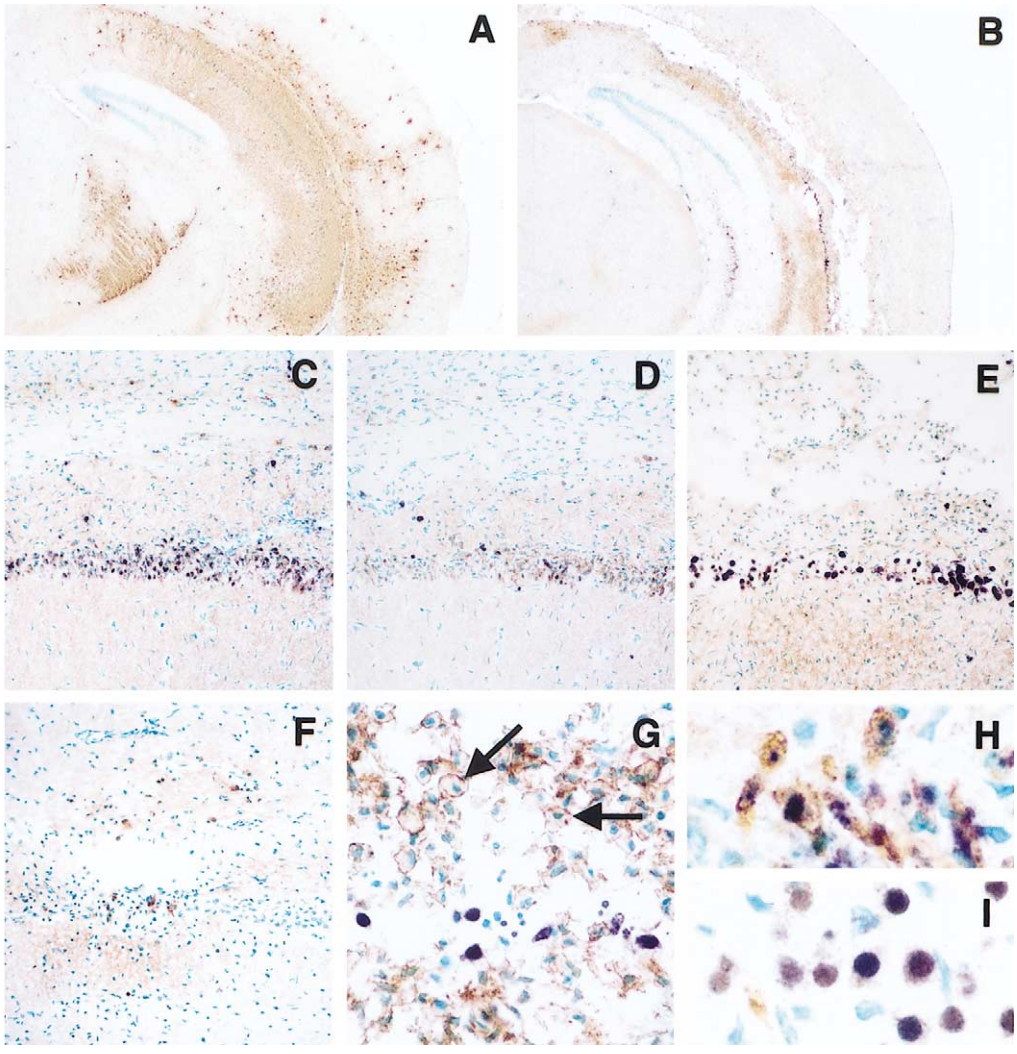

5

Table 1
Hippocampal lesions 20 days after intracerebral infection with NSV followed by passive transfer of immune serum

Mouse strain	No. of survivors/total	No. of mice with the histological grades of hippocampal lesion			
		NSL[a]	Mild[b]	Severe[c]	P[d]
C57BL/6	7/10	2	0	5	—
CD4-KO	8/10	1	7	0	<0.01
CD8-KO	8/10	2	2	4	NS
IFG-KO	8/10	1	3	4	NS
RAG-KO	9/10	1	5	3	NS

[a] No significant lesions in hippocampus.
[b] Thinning and focal loss of pyramidal cell layer.
[c] Extensive loss of pyramidal cell layer.
[d] Fisher's exact test comparing severe lesions to C57BL6 mice; NS = not significant.

performed histopathological analysis on two or three mice each day at 1, 3, 7, 10, 13, 16, 20, 25, 30, and 62 days after infection. Mice autopsied at each time point showed similar histological findings and the disease process appeared to follow a rigid time course. The most prominent histological changes were the loss of the CA1 and CA2 regions of the hippocampal gyrus (Figs. 4A and B). Histopathological changes were initially observed in the CA1 pyramidal layer. At 3 days after infection, the majority of pyramidal neurons in the CA1 region showed prominent swelling of nuclei (Fig. 4D) compared with pyramidal neurons of uninfected mice (Fig. 4C). Cytoplasmic swelling was occasionally seen. White matter adjacent to the hippocampus (alveus and tapetum) was slightly edematous and minute hemorrhages were frequently observed. From days 7 to 13, many pyramidal neurons in CA1 and CA2 developed shrunken, eosinophilic cytoplasm and pycnotic or fragmented nuclei (Figs. 4E and F). A small number of dead neurons was also noted in CA3 on days 13 and 16. The number of dead neurons present decreased after day 16 with the loss of hippocampal tissue.

Increased cellularity of CA1, CA2, and the adjacent white matter indicative of an inflammatory response was first detectable at day 7 (Fig. 4E), reached a maximum on day 10 to day 13 (Figs. 4F and G), and then gradually decreased. The first signs of malacic changes were seen at day 10 with infiltration of activated foamy macrophages. Breakdown of CA1, CA2, adjacent white matter, and deep cortex progressed rapidly, and cavitation was observed by day 13 (Fig. 4G) and completed by day 20 (Figs. 4B and K). The resulting large cavities connected to the lateral ventricles, became fluid-filled, and appeared as hydrocephalus. The cavitation did not progress further and cavities eventually were lined with ependymal cells (Fig. 4H). Mild astrocytosis was present around the cavities and rarefaction was present in the basal zone of the cerebral cortex. Malacic changes also occurred at the junction of the corpus callosum (genu and truncus) and fornix superior, resulting in communication between the right and left lateral ventricles.

Since hydrocephalus is most frequently caused by obstruction of the flow of cerebrospinal fluid, the ventricular system was analyzed. A focal denuding of ependymal cells lining the lateral ventricular surface was observed from day 3 to day 10. The ependymal lining was repaired by day 13 and a proliferation of subependymal glia was associated with sites of ependymal damage. Ependymal cells lining the third ventricle and aqueduct were not affected. By histological analysis, neither the aqueduct of Sylvius nor the foramina of Monro was occluded.

In addition to the lesions described above, glial nodules and perivascular mononuclear cell infiltration were observed by day 7 in the cerebral cortex and thalamus and remained until last examined at day 62. Uninfected control mice intracerebrally inoculated with HBSS and then intraperitoneally inoculated with immune sera did not develop pathologic changes (Figs. 4A and C).

RAG-KO mice, infected with NSV and rescued by immune serum, showed reappearance of infectious virus by

Fig. 1. Pathologic changes in the brains of mice surviving NSV infection. Coronal sections of an infected (A) and uninfected (B) C57BL/6 mouse. Hematoxylin and eosin stain. Eleven-week-old mice were infected intracerebrally with 1000 PFU of NSV. Two months later brains of mice that survived acute encephalitis were examined. In NSV-infected mice (A) the CA1 pyramidal layer (asterisk in B) and surrounding parenchymal tissue were lost and the lateral ventricle was markedly dilated. Magnification: ×18.

Fig. 5. Characterization of TUNEL-positive cells. Double staining of NSV (brown) and TUNEL (dark blue) in the brains of B6 mice (A, B, C, E, H, and I) and RAG-KO mice (D and F) rescued from fatal NSV infection by passive transfer of immune serum. (G) Double staining of F4/80 Ag (brown) and TUNEL (dark blue) in a B6 mouse. Virus Ag distribution at 3 days (A) and 16 days (B) after infection. At 7 days after infection, infected pyramidal cells showed TUNEL-positivity in B6 mice (C) and RAG-KO mice (D). On day 13, many TUNEL-positive cells were observed in the pyramidal layer of B6 mice (E) but not in RAG-KO mice (F). At 7 days (C) and 10 days (H) after infection, TUNEL-positive pyramidal neurons in B6 mice showed immunoreactivity for NSV. A majority of TUNEL-positive neurons in B6 mice on day 13 (E) and day 16 (I) did not show NSV immunoreactivity. (G) Infiltrating activated macrophage/microglial cells (arrows) and TUNEL-positive pyramidal neurons on day 13. Magnification: A, ×17; B, ×16; C, D, E, and F, ×110; G, ×330; H and I, ×778.

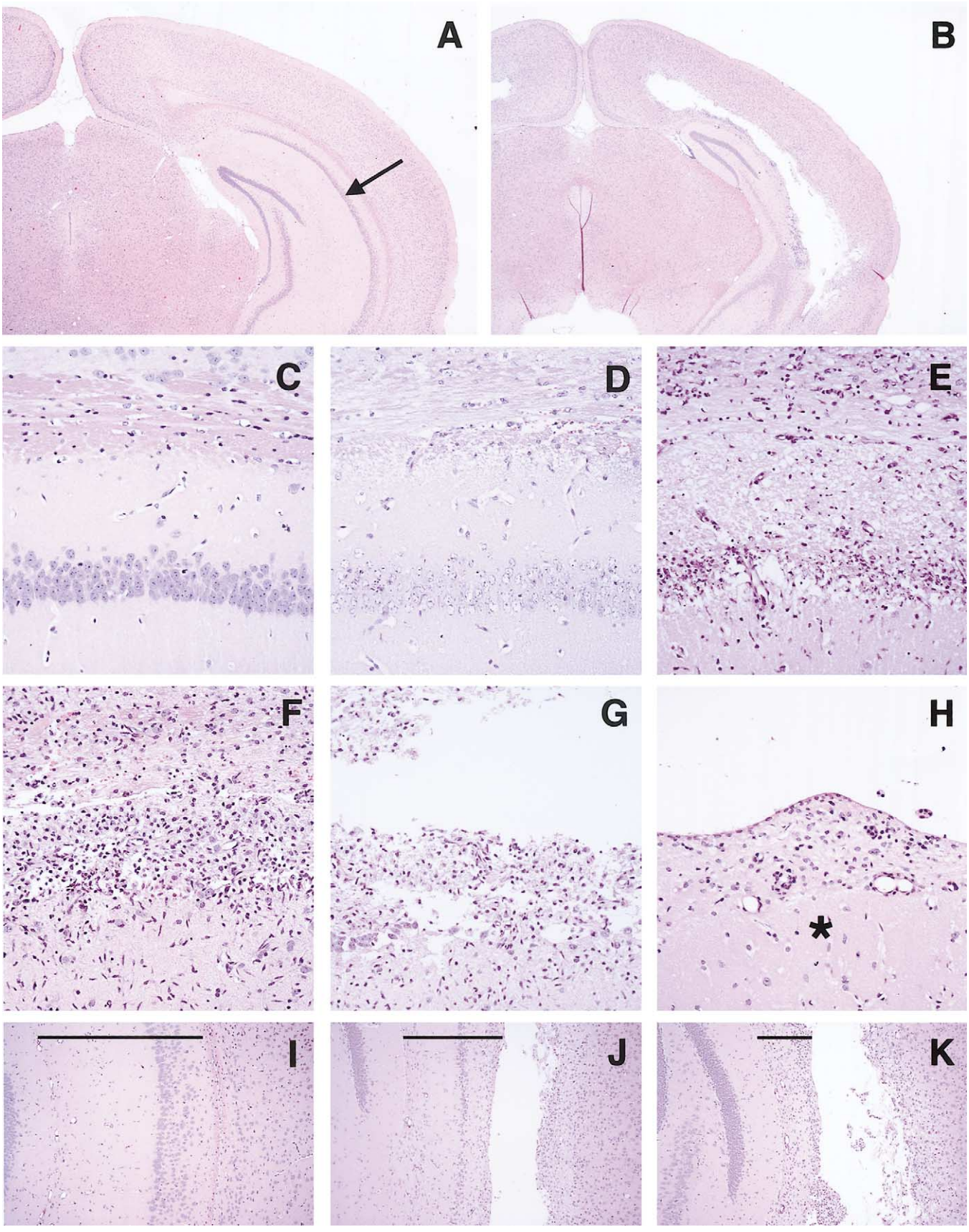
A
B
C
D
E
F
G
H
*
I
J
K

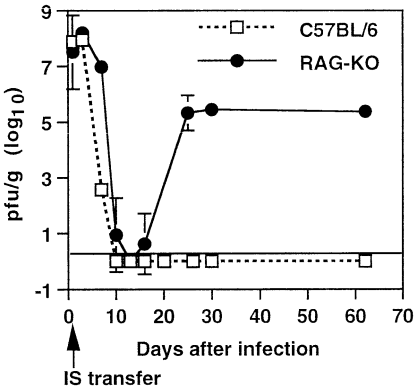

Fig. 2. Replication of NSV in the brains of immunocompetent and RAG-KO B6 mice. Mice infected intracerebrally with 1000 PFU NSV were treated intraperitoneally with 0.2 ml of NSV immune serum (IS) 24 h after infection. Bars represent one standard deviation.

day 16 (Fig. 2) and were expected to show evidence of virus-induced damage. Histological findings on day 3 were quite similar to those of B6 mice, but between day 7 and day 20 fewer mononuclear cells infiltrated the hippocampus and adjacent white matter in RAG-KO mice than in B6 mice. Malacic changes and cavitation in RAG-KO mice (Fig. 4J) were often milder than in B6 mice (Fig. 4K) and hydrocephalus was less extensive.

Virus distribution and colocalization with TUNEL-positive cells

To determine whether dying neurons were infected with NSV, brains were stained for both virus antigen and DNA fragmentation. Three days after infection virus was present in the CA1 region of the hippocampus, adjacent white matter, and deep cortex and a majority of pyramidal neurons was positive for viral antigen (Fig. 5A). In CA1, viral antigen was present in the neuropil as well as in the cytoplasm of pyramidal neurons. Viral antigen was also detected in the cytoplasm of glial cells in white matter adjacent to the hippocampus and corpus callosum. Foci of infected neurons were scattered throughout the cerebral cortex, basal ganglia, thalamus, and brain stem. Clearance of viral antigen was apparent by day 7 and was more rapid from the cerebral cortex and thalamus than from the hippocampus (Fig. 5B). Viral antigen was still detected in the CA1 neuropil on day 20. In RAG-KO mice, a few antigen-positive neurons were detected in cerebral cortex, thalamus, and basal ganglia on day 30 and day 62 (data not shown).

Infected neurons had no TUNEL reactivity at day 3 (Fig. 5A). By 7 days after infection TUNEL-positive neurons were present in the pyramidal layer in both RAG-KO and B6 mice (Figs. 5C and D) and most were also positive for viral antigen (Fig. 5H). TUNEL-reactivity of infected neurons was similar in B6 mice and RAG-KO mice at day 10 (Figs. 5C and D), but differences were present later (Figs. 5E and F). In B6 mice, many TUNEL-positive cells were observed in the CA1 and CA2 pyramidal layers 13-16 days after infection when the number of viral antigen-positive cells was markedly decreased (Fig. 5E), and a majority of the TUNEL-positive cells were negative for viral antigen (Fig. 5I). In RAG-KO mice there were fewer TUNEL-positive cells in the pyramidal layer 13-16 days after infection than at earlier times (Figs. 5D and F). The numbers of TUNEL-positive cells in both B6 mice and RAG-KO mice decreased rapidly after day 16. In RAG-KO mice the few antigen-positive neurons scattered in cerebral gray matter from day 20 to 62 were not TUNEL-positive.

A possible source of apoptotic cells observed in the pyramidal layers was infiltrating mononuclear cells. These cells were excluded from analysis by a variety of criteria. The few apoptotic lymphocytes present within the pyramidal layer and could be excluded from the count by their shape and small size compared to neurons. SV does not replicate in mononuclear cells in vivo or in vitro (Griffin and Johnson, 1973; Johnson, 1965) so lymphocytes will not be positive for both TUNEL and SV antigen. Double labeling for TUNEL-positive nuclei and F4/80 antigen (Fig. 5G) revealed that less than 5% of TUNEL-positive cells within the pyramidal layer were macrophage/microglia, indicating that the majority of TUNEL-positive cells were pyramidal neurons.

Virus antigen and TUNEL-positive cells were not detected at any time point in the brains of control mice intracerebrally inoculated with HBSS and then given immune serum.

Differences in the severity of hippocampal lesions between strains of immunodeficient mice

To identify the component of cellular immunity involved in the development of hydrocephalus, mice that genetically lack CD4 (CD4-KO), CD8 (CD8-KO), and IFN-γ (IFG-KO) were infected with NSV and treated with NSV immune

Fig. 4. Ex vacuo hydrocephalus in mice rescued from fatal NSV infection by passive transfer of immune serum. Coronal sections of uninfected mice (A and C), NSV-infected B6 mice (B, D, E, F, G, H, and K), NSV-infected CD4-KO mice (I), and NSV-infected RAG-KO mice (J). Hematoxylin and eosin stain. All mice were treated with immune serum 24 h after infection. CA1 pyramidal layer (arrow in A) was lost in B6 mice by 20 days after infection (B). Panels C, D, E, F, G, and H show the CA1 pyramidal layer at higher magnification. Compared with uninfected mice (C), swelling of pyramidal neurons was prominent at 3 days (D) after infection. Death of pyramidal neurons and mononuclear cell infiltration on day 7 (E) and day 10 (F) were followed by cavitation on day 13 (G). The thinned CA1 region was covered with ependymal cells by day 62 (H). The asterisk indicates the dentate gyrus. Bars in panel I (no significant lesion), J (mild lesion), and K (severe lesion) represent the thickness of CA1 at 20 days after infection and the measurement used for scoring hippocampal damage. Magnification: A and B, ×11; C, D, E, F, G, and H, ×110; I, J, and K, ×35.

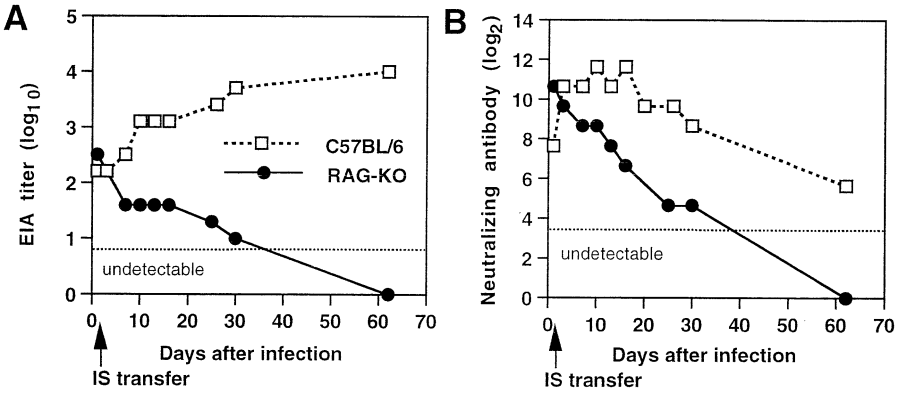

Fig. 3. Antibody responses of immunocompetent and RAG-KO B6 mice. (A) EIA-reactive anti-SV antibody; (B) neutralizing antibody. Mice infected intracerebrally with 1000 PFU NSV were treated intraperitoneally with 0.2 ml of NSV immune serum (IS) 24 h after infection.

serum 24 h later. Since the loss of hippocampal tissue leads to cavitation, we compared the severity of hippocampal loss of these selectively immunodeficient mice with that of immunocompetent B6 mice at day 20 when hydrocephalus was fully developed (Table 1). The extent of hippocampal loss is reflected in the thickness of the CA1 region and this measurement was used to grade and score the degree of hippocampal damage (Fig. 4I, no significant lesion; Fig. 4J, mild lesion; Fig. 4K, severe lesion). No surviving CD4-KO mice developed severe hippocampal lesions, while 71% of immunocompetent B6 mice ($P < 0.01$), 50% of CD8-KO, 50% of IFG-KO mice, and 33% of RAG-KO mice developed severe lesions.

Effect of T cell depletion on the death of hippocampal pyramidal neurons

Since mononuclear cell infiltration was closely associated with hippocampal loss and the development of cavitation (Fig. 4), we analyzed the relationship between the number of infiltrating mononuclear cells and the TUNEL-positive cells in the hippocampal gyrus. Mice were selectively depleted of T cells by inoculation with anti-CD4 monoclonal antibody (MAb), anti-CD8 MAb, or normal rat serum. No surviving anti-CD4 MAb-treated mice developed severe hippocampal lesions, while 80% of anti-CD8 MAb-treated mice and 83% of normal rat serum-treated mice developed severe lesions ($P < 0.05$) (Table 2). One-third of the mice treated with both anti-CD4 and anti-CD8 MAbs showed severe lesions.

Fewer F4/80-positive (macrophage/microglial) cells were present 13 days after infection in mice treated with anti-CD4 MAbs than in untreated mice ($P < 0.02$) (Fig. 6A). Few CD4-positive cells were detected in mice treated with anti-CD4 MAb (Fig. 6B), and these cells resembled ramified microglia morphologically. No CD8-positive cells were detected in mice treated with anti-CD8 MAb (Fig. 6C). More TUNEL-positive cells were observed in untreated mice than mice treated with anti-CD4 MAb on day 13 ($P < 0.05$) but not on day 10 (Fig. 6D). Differences between mice treated with anti-CD8 MAb, anti-CD4 MAb, and the mixture of anti-CD4 and anti-CD8 MAbs were not significant.

Discussion

Mice surviving NSV infection developed hydrocephalic changes over the course of 3 weeks as a result of progressive loss of tissue from the hippocampal gyrus, adjacent white matter, and deep cerebral cortex despite the clearance

Table 2
Effect of T cell depletion on the development of hippocampal lesions in C57BL/6 mice 20 days after intracerebral infection with NSV followed by passive transfer of immune serum

Treatment	No. of survivors/total	No. of mice with the histological grades of hippocampal lesion			
		NSL[a]	Mild[b]	Severe[c]	P[d]
Normal rat serum	6/6	1	0	5	—
Anti-CD4	4/6	2	2	0	<0.05
Anti-CD8	5/6	0	1	4	NS
Anti-CD4 + Anti-CD8	6/6	2	2	2	NS

[a] No significant lesions in hippocampus.
[b] Thinning and focal loss of pyramidal cell layer.
[c] Extensive loss of pyramidal cell layer.
[d] Fisher's exact test comparing severe lesions to normal rat serum control; NS = not significant.

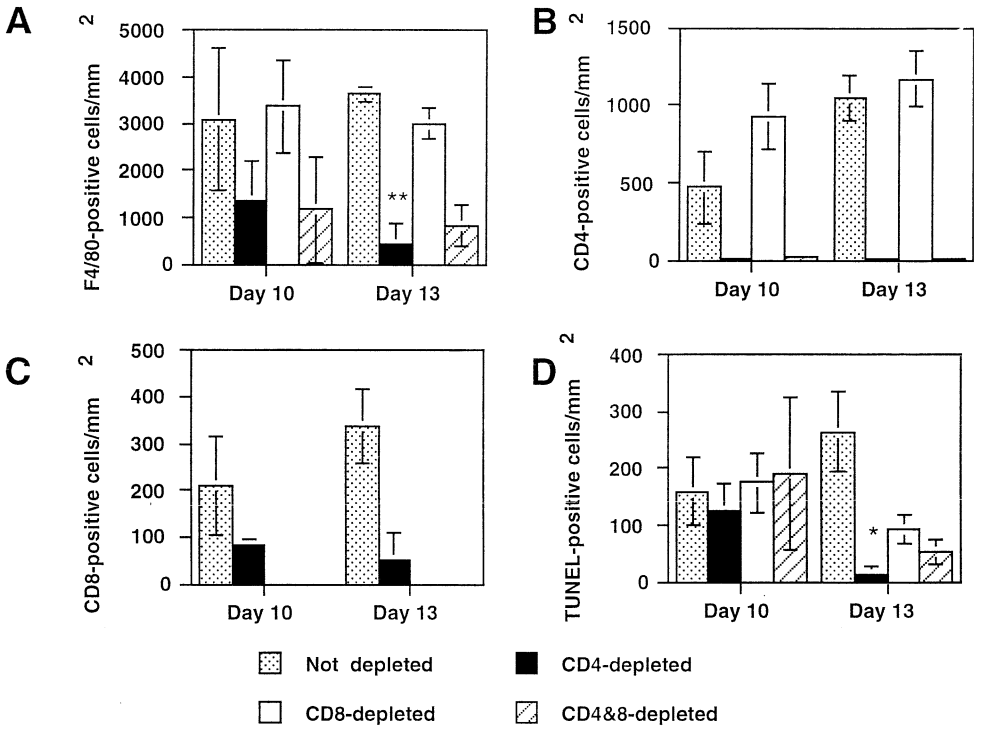

Fig. 6. Correlation of the numbers of infiltrating mononuclear cells with TUNEL-positive cells in the hippocampus. (A) F4/80-positive cells (macrophage/microglia), (B) CD4-positive cells, and (C) CD8-positive cells infiltrating the hippocampal gyrus of normal and T cell depleted mice were counted as described under Materials and methods. The number of TUNEL-positive cells (D) are the positive cells within hippocampal pyramidal cell layers. Bars represent standard errors of the mean. $^{**}P < 0.02$, $^{*}P < 0.05$, Student's t test.

of infectious virus within 10 days after infection. Progressive histopathologic changes were observed when death from acute fatal encephalomyelitis was prevented by passive transfer of immune serum after CNS infection had been established. Mice lacking CD4 T cells had hippocampal damage that was less extensive and had fewer macrophages infiltrating areas of virus-infected cells. The data suggest the possibility that $CD4^+$ T cells responding to viral antigen in the CNS promote the recruitment and activation of macrophages that contribute to progressive regional neuronal death and tissue injury despite clearance of infectious virus.

Hydrocephalus is a relatively unusual outcome of viral encephalitis, but CNS infection with a variety of viruses, such as herpes simplex (Hayashi et al., 1986; Schinazi and Yao, 1995), measles (Haspel and Rapp, 1975), mumps (Johnson et al., 1967), Ross River (Mims et al., 1973), Sendai (Kristensson et al., 1984), and Theiler's murine encephalitis (Tsunoda et al., 1997) viruses occasionally induces hydrocephalus in rodents. In all of these viral infections hydrocephalus results from abnormalities in cerebrospinal fluid flow associated with inflammation at sites of ependymal or meningeal infection that may lead to aqueductal stenosis and macrocephaly. The pathogenesis of hydrocephalus in NSV-infected mice was a consequence of massive tissue destruction resulting in dilatation of the lateral ventricles and "ex vacuo" hydrocephalus.

The CA1 region of the hippocampus was particularly vulnerable to NSV infection and progressive tissue destruction. The hippocampus is a target for other viral infections, such as Borna disease virus (Hirano et al., 1983) and rabies virus (Jackson and Rossiter, 1997) and is particularly prone to neurodegenerative damage in many experimental systems of neuronal injury. In measles virus encephalitis in BALB/c mice hippocampal pyramidal cell damage in the CA1 and CA3 regions is secondary to excitotoxic injury associated with infection of cortical neurons (Love et al., 1986; Andersson et al., 1993), while in NSV encephalitis in C570L/6 mice direct infection is involved. NSV infects a wide variety of neurons in the cortex and brainstem as well as the hippocampus, but extensive progressive damage was limited to the hippocampus and adjacent areas of the cortex and corpus callosum.

Early in NSV infection, the hippocampal gyrus, adjacent white matter, and deep cerebral cortex were extensively infected and NSV-positive pyramidal neurons showed TUNEL reactivity. Infection was controlled and infectious virus was cleared prior to progressive damage, but viral antigen persisted. Limited virus replication may contribute to ongoing neurodegeneration through mechanisms related to decreased neuronal Na^+K^+ATPase activity or local release of excitotoxic amino acids (Lees and Leong, 1996; Lees et al., 1990; Nargi-Aizenman and Griffin, 2001; Nargi-Aizenman et al., unpublished observations). SV directly affects the function of Na^+K^+ATPase in infected cells

(Ulug et al., 1984; Garry et al., 1979; Despres et al., 1995) and dying neurons may release glutamate (Nargi-Aizenman and Griffin, 2001). The number of NSV-positive pyramidal cells decreased with the clearance of infectious virus, but death of virus antigen-negative pyramidal neurons and malacic changes were progressive. Progressive damage after clearance of infectious virus has also been observed in the retina of MHV-infected mice associated with persistence of viral RNA (Komurasaki et al., 1996). In a variety of cell lines, SV infection activates a programmed cell death pathway resulting in apoptosis (Levine et al., 1993; Nava et al., 1998; Ubol et al., 1994). The relatively neurovirulent TE strain of SV induces apoptosis in neurons of 2-week-old mice (Lewis et al., 1996) and the current studies indicate that infection of pyramidal cells of the hippocampus with NSV also caused nuclear DNA fragmentation typically observed in apoptotic cell death.

This study also showed that extensive loss of hippocampal pyramidal cells is unrelated to mortality. Mice receiving transferred immune sera did not show hindlimb paralysis, a characteristic neurological sign of NSV-induced encephalomyelitis (Jackson et al., 1987), while this was observed after reappearance of infectious virus in RAG-KO mice. In contrast to hippocampal pyramidal neurons, large spinal cord motor neurons in the ventral horn were free of virus at the time of immune serum transfer, which probably prevented spread of virus infection to the spinal cord. Although hydrocephalic mice did not show gross neurological deficits, higher neurological functions such as learning and memory are likely to have been affected. Passive transfer of immune serum offers protection from fatal acute disease, but also increases the likelihood of delayed or chronic neurological disease. For instance, subacute encephalitis can be established in mice infected with measles virus that have received passively transferred antibody, a process postulated to be related to the development of the human progressive neurological disease subacute sclerosing panencephalitis (Rammohan et al., 1981). Mice receiving immune serum after peripheral inoculation of Semliki Forest virus develop a delayed onset of encephalitis (Seamer et al., 1971). Passive transfer of antibody may contribute to disease by affecting the induction of the primary antiviral immune response in poorly understood ways.

Virus antigen remained in the neuropil of the hippocampal gyrus up to day 20. These findings suggest that viral clearance from the processes of pyramidal cells may be slower than from their cell bodies. An alternative explanation is that virus antigen-containing processes remained for a time after the death of the neuron. Mononuclear cell infiltration persisted after clearance of infectious virus, suggesting that virus antigen continues to attract and retain mononuclear cells.

Many TUNEL-positive pyramidal neurons observed after the clearance of infectious virus from brain were virus antigen-negative. This phase of neuronal cell death appeared to be immune-mediated because virus antigen-negative, TUNEL-positive neurons were rare in RAG-KO and CD4-depleted mice. Although neuronal death was temporally related to the infiltration of $CD4^+$ T cells and macrophages, dead neurons were not always in immediate contact with mononuclear cells. This suggests that cell death may be caused by a soluble factor produced by $CD4^+$ T cells or macrophages rather than by direct contact with these mononuclear cells.

The numbers of macrophage/microglia cells infiltrating the hippocampal gyrus were significantly greater in immunocompetent mice than mice lacking $CD4^+$ T cells. $CD4^+$ T cells may play an important role in recruitment of mononuclear cells into the region and in the development of hydrocephalic changes. The role of macrophages in tissue injury may be more important than the role of CD4 T cells because some mice lacking CD4 and CD8 T cells developed macrophage infiltration and severe hippocampal loss. This finding also suggests a protective role for CD8 T cells in tissue injury.

Activated macrophages and microglia can produce a number of factors toxic to neurons including glutamate and other excitotoxins (Giulian et al., 1993, 1996; Wood, 1995; Lees, 1993; Flavin et al., 1997) and cytokines, such as tumor necrosis factor and interleukin-1β (Fine et al., 1997). $CD4^+$ T cells are implicated in inducing damage; however, IFN-γ does not appear to be directly important because IFG-KO mice also developed severe hippocampal loss. In addition to glutamate and cytokines, macrophage/microglia can produce a variety of other neurotoxic factors (Mercurio and Shaw, 1988; Flavin et al., 1997; Giulian et al., 1996) and cause delayed neuronal loss in ischemic and traumatic CNS lesions (Giulian et al., 1993; Lees, 1993; Wood, 1995). Reactive microglia and macrophages may also contribute to CNS damage during and after acute viral encephalomyelitis.

Materials and methods

Virus and mice

NSV (Griffin and Johnson, 1977) used in this study was harvested from infected BHK-21 cells. Mice homozygous for a targeted disruption of the CD4 gene (C57BL/6-$Cd4^{tm1Mak}$), the CD8α gene (C57BL/6-$Cd8a^{tm1Mak}$), the interferon-γ gene (C57BL/6-$Ifng^{tm1Ts}$), the recombination activating gene-1 (C57BL/6J-$Rag1^{tm1Mom}$), and syngeneic C57BL/6J mice were purchased from the Jackson Laboratory (Bar Harbor, ME). All studies were approved by the Animal Care and Use Committee of the Johns Hopkins University.

Infection of mice, serum transfer, and tissue processing

For production of anti NSV serum, female B6 mice, 6-8 weeks old, were inoculated subcutaneously with 2×10^5 PFU NSV in 30 μl HBSS distributed between the hind feet.

Blood was collected 2 weeks after immunization by cardiac puncture under anesthesia, and sera from 20 to 50 mice were pooled. Pooled sera had a neutralizing titer of 1:6400 as measured by the 50% plaque reduction test.

For infection, 6-week-old female mice under anesthesia were inoculated intracerebrally with 1000 PFU of NSV in 30 μl HBSS. Some mice were given 0.2 ml of immune serum intraperitoneally 24 h after infection. At various times after infection, groups of three to six mice were anesthetized and perfused with PBS. For virus titration, brains were quickly removed and frozen in liquid nitrogen. For histology, mice were further perfused with 0.5% periodate-lysine-paraformaldehyde (Gendelman et al., 1983; McLean and Nakane, 1974) or 4% paraformaldehyde. Periodate-lysine-paraformaldehyde-fixed tissue was placed in 0.5 M sucrose overnight at 4°C and then snap frozen in dry ice-cooled isopentane. Paraformaldehyde-fixed tissue was embedded in paraffin.

Virus titration

Brains were thawed and 33% homogenates were prepared with PBS as a diluent. Virus content in each homogenate was determined by plaque formation of serial 10-fold dilutions on BHK-21 cells. The geometric mean of data obtained from the tissues of two to three mice was determined for each time point.

Antibody measurement

Sera were collected by cardiac puncture under anesthesia and pooled from groups of four mice. Anti-SV binding antibody was measured by EIA (Stanley et al., 1985). Data are expressed as the highest dilution giving a value two times the background optical density observed with normal mouse serum. Neutralizing antibody was measured by the 50% plaque reduction test in BHK-21 cells.

Immunohistochemistry

Immunohistochemistry was performed using the avidin-biotinylated enzyme-complex method (Hsu et al., 1981) with modifications. Frozen tissues were embedded in Tissue-Tek O.C.T. compound (Sakura Finetek U.S.A., Torrance, CA) and cryosectioned. Sections were treated with 0.03% H_2O_2 in PBS for 5 min to block endogenous peroxidase activity, further blocked with the avidin-biotin blocking kit (Zymed, South San Francisco, CA), and then with 0.5% non-fat dried milk in PBS for 30 min. Primary antibodies consisted of a rabbit anti-SV IgG, a rat anti-mouse CD4 MAb (1:1000; clone RM4-5, Pharmingen, San Diego, CA), a rat anti-mouse CD8α MAb (1:100; clone KT15, Serotec, Kidlington, Oxford, UK), and a rat anti-mouse F4/80 MAb (1:100; Serotec). Sections were incubated for 30 min. After washing with PBS, sections stained for SV antigen were incubated with biotinylated goat anti-rabbit IgG (Vector Laboratories, Burlingame, CA) for 30 min, and sections stained for CD4, CD8α, or F4/80 antigens were incubated with a 1:100 dilution of biotinylated rabbit anti-rat IgG (Vector) for 30 min. Immunolabeled cells were visualized by VECTASTAIN Elite ABC kit (Vector) and 3,3′-diaminobenzidine tetrachloride according to the manufacturer's protocol. Sections were counterstained with methyl green, dehydrated, rinsed in Histo-Clear (National Diagnostics, Atlanta, GA), and mounted in Permount (Fisher).

Immunolabeled mononuclear cells infiltrating the hippocampal gyrus were counted using a Nikon Eclipse E800 microscope under ×40 objective. The coronal sections used for counting were just posterior to the attachment of the pituitary. This section includes the cerebral cortex, the thalamus, the third ventricle, and the hippocampal CA1, CA2, and CA3 regions. Ten areas were selected at random from the entire CA1 and CA2 regions of each section and counted. Values from the brains of two to three mice were averaged for each time point.

Terminal deoxynucleotidotransferase-mediated dUTP nick end-labeling (TUNEL) frozen and paraffin-embedded sections were treated with 1% H_2O_2 in methanol for 30 min and then with avidin–biotin blocking kit (Zymed). Sections were incubated with 40 μl of labeling mixture consisting of 200 mM potassium cacodylate, 25 mM Tris–HCl pH 6.6, 0.25 mg/ml BSA, 2 mM cobalt chloride, 1 μM biotin-16-dUTP (Boehringer Mannheim, Indianapolis, IN), and 0.125 unit/μl terminal transferase (Boehringer Mannheim) at 37°C for 1 h. The reaction was terminated by incubation in 2× SSC at room temperature for 15 min. After washing with PBS, sections were blocked in 2% bovine serum albumin for 10 min, and VECTASTAIN ABC-AP kit (Vector) was used for detection of incorporated biotin. Alkaline phosphatase conjugated avidin–biotin complexes were visualized with a solution containing 4-nitroblue tetrazolium chloride (Boehringer Mannheim), X-phosphate (Boehringer Mannheim), and levamisole (Vector) according to the manufacturer's protocol. For simultaneous detection of TUNEL reactivity and SV antigen, sections were then stained for virus, counterstained, dehydrated, and mounted as described above.

TUNEL-positive cells within the pyramidal cell layer were counted under a ×40 objective. Coronal sections just posterior to the attachment of the pituitary were analyzed. Twenty areas of the pyramidal cell layer were selected at random from the entire CA1 and CA2 regions of each section and counted. Values from the brains of four to six mice were averaged for each time point. To minimize the possibility of counting apoptotic mononuclear cells, the small numbers of TUNEL-positive cells with lymphocyte morphology were disregarded in the analysis.

T cell depletion

MAbs against mouse CD4 (clone GK 1.5) (Wofsy et al., 1985) or CD8 (clone 2.43; American Type Culture Collection, Manassas, VA) (Sarmiento et al., 1980) were produced as ascitic fluid in ICR-*scid* mice (Taconic, NY). The IgG2b concentration was measured by EIA using rat IgG2b as a standard. For depletion 0.25 mg of MAb was injected intraperitoneally 5, 4, and 3 days before and 1, 6, and 11 days after infection with NSV. Depletion (>97%) was confirmed by flow cytometry analysis of spleen cell suspensions in each mouse.

Acknowledgments

We thank Michael B. Havert, Gwendolyn K. Binder, and Jennifer L. Nargi-Aizenman for helpful discussions. This work was supported by Grants NS18596 and NS38932 from the National Institutes of Health (D.E.G.) and by Hokkaido University (T.K.).

References

Andersson, T., Schwarcz, R., Love, A., Kristensson, K., 1993. Measles virus-induced hippocampal neurodegeneration in the mouse: a novel, subacute model for testing neuroprotective agents. Neurosci. Lett. 154, 109–112.

Bilzer, T., Stitz, L., 1994. Immune-mediated brain atrophy. CD8+ T cells contribute to tissue destruction during borna disease. J. Immunol. 153, 818–823.

Binder, G., Griffin, D., 2001. Interferon-γ-mediated site specific clearance of alphavirus from CNS neurons. Science 293, 303–306.

Despres, P., Griffin, J.W., Griffin, D.E., 1995. Effects of anti-E2 monoclonal antibody on Sindbis virus replication in AT3 cells expressing bcl-2. J. Virol. 69, 7006–7014.

Fine, S.M., Angel, R.A., Perry, S.W., Epstein, L.G., Rothstein, J.D., Dewhurst, S., Gelbard, H.A., 1997. Tumor necrosis factor alpha inhibits glutamate uptake by primary human astrocytes: implications for pathogenesis of HIV-1 dementia. J. Biol. Chem. 271, 15303–15306.

Flavin, M., Coughlin, K., Ho, L., 1997. Soluble macrophage factors trigger apoptosis in cultured hippocampal neurons. Neuroscience 80, 437–448.

Garry, R.F., Bishop, J.M., Park, S., Westbrook, K., Lewis, G., Waite, M.R.F., 1979. Na+ and K+ concentrations and the regulation of protein synthesis in Sindbis virus-infected chick cells. Virology 96, 108–120.

Gendelman, H.E., Moench, T.R., Narayan, O., Griffin, D.E., 1983. Selection of a fixative for identifying T cell subsets, B cells and macrophages in paraffin-embedded mouse spleen. J. Immunol. Methods 65, 137–145.

Giulian, D., Corpuz, M., Chapman, S., Mansouri, M., Robertson, C., 1993. Reactive mononuclear phagocytes release neurotoxins after ischemic and traumatic injury to the central nervous system. J. Neurosci. Res. 15, 681–693.

Giulian, D., Yu, J., Li, X., Tom, D., Li, J., Wendt, E., Lin, S., Schwarcz, R., Noonan, C., 1996. Study of receptor-mediated neurotoxins released by HIV-1-infected mononuclear phagocytes found in human brain. J. Neurosci. 15, 3139–3153.

Griffin, D.E., 1976. Role of the immune response in age-dependent resistance of mice to encephalitis due to Sindbis virus. J. Infect. Dis. 133, 456–464.

Griffin, D.E., Johnson, R.T., 1973. Cellular immune response to viral infection: in vitro studies of lymphocytes from mice infected with Sindbis virus. Cell. Immunol. 9, 426–434.

Griffin, D.E., Johnson, R.T., 1977. Role of the immune response in recovery from Sindbis virus encephalitis in mice. J. Immunol. 118, 1070–1075.

Haspel, M.V., Rapp, F., 1975. Measles virus: an unwanted variant causing hydrocephalus. Science 187, 450–451.

Hayashi, K., Iwasaki, Y., Yanagi, K., 1986. Herpes simplex virus type 1-induced hydrocephalus in mice. J. Virol. 57, 942–951.

Hirano, N., Kao, M., Ludwig, H., 1983. Persistent, tolerant or subacute infection in Borna disease virus-infected rats. J. Gen. Virol. 64, 1521–1530.

Hirsch, R.L., Griffin, D.E., Johnson, R.T., 1979. Interactions between immune cells and antibody in protection from fatal Sindbis virus encephalitis. Infect. Immunity 23, 320–324.

Hsu, S.M., Raine, L., Fanger, H., 1981. The use of avidin-biotin-peroxidase-complex (ABC) in immunoperoxidase techniques: a comparison between ABC and unlabeled antibody (PAP) procedures. J. Histochem. Cytochem. 29, 577–580.

Jackson, A.C., Moench, T.R., Griffin, D.E., 1987. The pathogenesis of spinal cord involvement in the encephalomyelitis of mice caused by neuroadapted Sindbis virus infection. Lab. Invest. 56, 418–423.

Jackson, A., Rossiter, J., 1997. Apoptosis plays an important role in experimental rabies virus infection. J. Virol. 71, 5603–5607.

Johnson, R., Johnson, K., Edmonds, C., 1967. Virus-induced hydrocephalus: development of aqueductal stenosis in hamsters after mumps infection. Science 1, 1066–1067.

Johnson, R.T., 1965. Virus invasion of the central nervous system: a study of Sindbis virus infection in the mouse using fluorescent antibody. Am. J. Pathol. 46, 929–943.

Johnson, R.T., McFarland, H.F., Levy, S.E., 1972. Age-dependent resistance to viral encephalitis: studies of infections due to Sindbis virus in mice. J. Infect. Dis. 125, 257–262.

Kimura, T., Griffin, D.E., 2000. The role of $CD8^+$ T cells and major histocompatibility complex class I expression in the central nervous system of mice infected with neurovirulent Sindbis virus. J. Virol. 74, 6117–6125.

Komurasaki, Y., Nagineni, C., Wang, Y., Hooks, J., 1996. Virus RNA persists within the retina in coronavirus-induced retinopathy. Virology 222, 446–450.

Kristensson, K., Leestma, J., Lundh, B., Norrby, E., 1984. Sendai virus infection in the mouse brain: virus spread and long-term effects. Acta Neuropathol. (Berl.) 63, 89–95.

Lees, G., 1993. The possible contribution of microglia and macrophages to delayed neuronal death after ischemia. J. Neurol. Sci. 114, 119–122.

Lees, G., Lehmann, A., Sandbert, M., Hamberger, A., 1990. The neurotoxicity of ouabain, a sodium-potassium ATPase inhibitor, in the rat hippocampus. Neurosci. Lett. 11, 159–162.

Lees, G., Leong, W., 1996. Interactions between excitotoxins and the Na+/K+-ATPase inhibitor ouabain in causing neuronal lesions in the rat hippocampus. Brain Res. 1, 145–155.

Levine, B., Griffin, D.E., 1992. Persistence of viral RNA in mouse brains after recovery from acute alphavirus encephalitis. J. Virol. 66, 6429–6435.

Levine, B., Hardwick, J.M., Trapp, B.D., Crawford, T.O., Bollinger, R.C., Griffin, D.E., 1991. Antibody-mediated clearance of alphavirus infection from neurons. Science 254, 856–860.

Levine, B., Huang, Q., Isaacs, J.T., Reed, J.C., Griffin, D.E., Hardwick, J.M., 1993. Conversion of lytic to persistent alphavirus infection by the Bcl-2 cellular oncogene. Nature 361, 739–742.

Lewis, J., Wesselingh, S.L., Griffin, D.E., Hardwick, J.M., 1996. Alphavirus-induced apoptosis in mouse brains correlates with neurovirulence. J. Virol. 70, 1828–1835.

Lipton, H.L., 1975. Theiler's virus infection in mice: an unusual biphasic disease process leading to demyelination. Infect. Immunity 11, 1147–1155.

Lipton, H.L., Dal Canto, M.C., 1976. Theiler's virus-induced demyelination: prevention by immunosuppression. Science 192, 62–64.

Love, A., Norrby, E., Kristensson, K., 1986. Measles encephalitis in rodents: defective expression of viral proteins. J. Neuropathol. Exp. Neurol. 45, 258–267.

McLean, I.W., Nakane, P.K., 1974. Periodate-lysine-paraformaldehyde fixative: a new fixative for immunoelectron microscopy. J. Histochem. Cytochem. 22, 1077–1083.

Mercurio, A.M., Shaw, L.M., 1988. Macrophage interactions with laminin: PMA selectively induces adherence and spreading of mouse macrophages on a laminin substratum. J. Cell Biol. 107, 1873–1880.

Mims, C.A., Murphy, F.A., Taylor, W.P., Marshall, I.D., 1973. Pathogenesis of Ross River virus infection in mice. I. Ependymal infection, cortical thinning, and hydrocephalus. J. Infect. Dis. 127, 121–128.

Nargi-Aizenman, J., Griffin, D., 2001. Sindbis virus-induced neuronal death is both necrotic and apoptotic and is ameliorated by *N*-methyl-D-aspartate receptor antagonists. J. Virol. 75, 7114–7121.

Nava, V.E., Rosen, A., Veliuona, M.A., Clem, R.J., Levine, B., Hardwick, J.M., 1998. Sindbis virus induces apoptosis through a caspase-dependent, CrmA-sensitive pathway. J. Virol. 72, 452–459.

Rammohan, K.W., McFarland, H.F., McFarlin, D.E., 1981. Induction of subacute murine measles encephalitis by monoclonal antibody to virus haemagglutinin. Nature 290, 588–589.

Rowell, J.F., Griffin, D.E., 2002. Contribution of T cells to mortality in neurovirulent Sindbis virus encephalomyelitis. J. Neuroimmunol. 127, 106–114.

Sarmiento, M., Glasebrook, A.L., Fitch, F.W., 1980. IgG or IgM monoclonal antibodies reactive with different determinants on the molecular complex bearing LYT 2 antigen block of T cell-mediated cytolysis in the absence of complement. J. Immunol. 125, 2665–2672.

Schinazi, R.F., Yao, X., 1995. Hydrocephalus induction in mice infected with herpes simplex virus type 2 after antiviral treatment. Antiviral Res. 28, 291–302.

Seamer, J.H., Boulter, E.A., Zlotnick, I., 1971. Delayed onset of encephalitis in mice passively immunized against Semliki Forest virus. Br. J. Exp. Pathol. 52, 408–414.

Stanley, J., Cooper, S.J., Griffin, D.E., 1985. Alphavirus neurovirulence: monoclonal antibodies discriminating wild-type from neuroadapted Sindbis virus. J. Virol. 56, 110–119.

Stanley, J., Cooper, S., Griffin, D.E., 1986. Monoclonal antibody cure and prophylaxis of lethal Sindbis virus encephalitis in mice. J. Virol. 58, 107–115.

Taylor, R.M., Hurlbut, H.S., Work, T.H., Kingsbury, J.R., Frothingham, T.E., 1955. Sindbis virus: a newly recognized arthropod-transmitted virus. Am. J. Trop. Med. Hyg. 4, 844–846.

Thach, D., Kimura, T., Griffin, D., 2000. Differences between C57BL/6 and BALB/cBy mice in mortality and virus replication after intranasal infection with neuroadapted Sindbis virus. J. Virol. 74, 6156–6161.

Tsunoda, I., McCright, I., Kuang, L., Zurbriggen, A., Fujinami, R.S., 1997. Hydrocephalus in mice infected with a Theiler's murine encephalomyelitis virus variant. J. Neuropathol. Exp. Neurol. 56, 1302–1313.

Tucker, P.C., Griffin, D.E., Choi, S., Bui, N., Wesselingh, S., 1996. Inhibition of nitric oxide synthesis increases mortality in Sindbis virus encephalitis. J. Virol. 70, 3972–3977.

Tyor, W.R., Wesselingh, S., Levine, B., Griffin, D.E., 1992. Long term intraparenchymal Ig secretion after acute viral encephalitis in mice. J. Immunol. 149, 4016–4020.

Ubol, S., Tucker, P.C., Griffin, D.E., Hardwick, J.M., 1994. Neurovirulent strains of alphavirus induce apoptosis in Bcl-2-expressing cells; role of a single amino acid change in the E2 glycoprotein. Proc. Natl. Acad. Sci. USA 91, 5202–5206.

Ulug, E.T., Waite, M.R.F., Bose Jr., H.R., 1984. Alterations in monovalent cation transport in Sindbis virus-induced chick cells. Virology 132, 118–130.

Weiner, L.P., 1973. Pathogenesis of demyelination induced by a mouse hepatitis virus (JHM virus). Arch. Neurol. 28, 298–303.

Wesselingh, S.L., Levine, B., Fox, R.J., Choi, S., Griffin, D.E., 1994. Intracerebral cytokine mRNA expression during fatal and nonfatal alphavirus encephalitis suggests a predominant type 2 T cell response. J. Immunol. 152, 1289–1297.

Wofsy, D., Mayes, D.C., Woodcock, J., Seaman, W.E., 1985. Inhibition of humoral immunity in vivo by monoclonal antibody to L3T4: studies with soluble antigens in intact mice. J. Immunol. 135, 1698–1701.

Wood, P., 1995. Microglia as a unique cellular target in the treatment of stroke: potential neurotoxic mediators produced by activated microglia. Neurol. Res. 17, 242–248.

Zlotnick, I., Peacock, S., Grant, D.P., Batter-Hatton, D., 1972. The pathogenesis of Western equine encephalitis virus (WEE) in adult hamsters with special reference to the long and short term effects on the CNS of the attenuated clone 15 variant. Br. J. Exp. Pathol. 53, 59–77.